Inorganic Chemistry
Article
pubs.acs.org/IC

Photochemistry of Tetrasulfur Tetranitride: Laser Flash Photolysis and Quantum Chemical Study

Elena A. Pritchina,[†,‡] Daria S. Terpilovskaya,[†,‡] Yuri P. Tsentalovich,[∥,‡] Matthew S. Platz,[§] and Nina P. Gritsan*,[†,‡]

[†]Institute of Chemical Kinetics and Combustion and [∥]International Tomography Center, Siberian Branch of the Russian Academy of Sciences, Novosibirsk, Russia

[‡]National Research University—Novosibirsk State University, Novosibirsk, Russia

[§]Department of Chemistry, The Ohio State University, Columbus, Ohio 43210, United States

Supporting Information

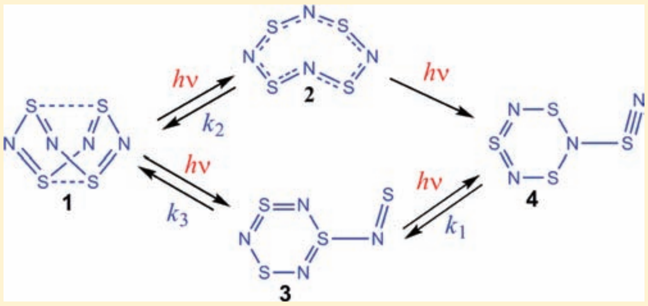

ABSTRACT: The photochemistry of tetrasulfur tetranitride (**1**) was studied in hexane solution by the laser flash photolysis technique (LFP). The experimental findings were interpreted using the results of previous matrix isolation studies (Pritchina, E.A.; Gritsan, N.P.; Bally, T.; Zibarev, A.V. *Inorg. Chem.* **2009**, *48*, 4075) and high-level quantum chemical calculations. LFP produces two primary intermediates, one of which is the boat-shaped 8-membered cyclic compound (**2**) and the other is the 6-membered S_3N_3 cyclic compound carrying an exocyclic (S)−N═S group (**3**). The primary products **2** and **3** absorb a second photon and undergo transformation to the 6-membered S_3N_3 cycle carrying an exocyclic (N)−S≡N group (**4**), which is very unstable and converts back to intermediate **3**. The quantum yield of the primary product formation is close to unity even though the quantum yield of photodegradation of **1** is low (~0.01). Thus, **1** is a photochromic compound undergoing in solution the thermally reversible photochemical isomerization. The mechanism of the photochromic process was established, and the rate constants of the elementary reactions were measured.

INTRODUCTION

The study of sulfur−nitrogen compounds, including both closed- and open-shell derivatives, is one of the most active areas of synthetic and structural inorganic chemistry.[1] Importantly, these compounds are widely used in the design and synthesis of functional molecular materials, in particular conducting, superconducting, and magnetic materials.[2−5] For instance, some open-shell sulfur−nitrogen derivatives and their selenium congeners isolated in the individual form reveal properties of conductors and low-temperature bulk ferromagnets and canted antiferromagnets.[2−5] The high and varied chemical reactivity of sulfur−nitrogen compounds is also far from being well-understood.[1,6]

Still one of the cornerstone compounds of the sulfur−nitrogen chemistry is tetrasulfur tetranitride (S_4N_4, **1**; Chart 1) first prepared in 1835.[1] Despite the fact that **1** is widely used in numerous inorganic and organoelement syntheses, its rich reactivity is not reliably interpreted (for discussion, see refs 7,8).

Chart 1

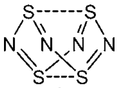

1

Compound **1** has a highly symmetric cage-structure (D_{2d}) in both the crystalline state and the gas phase.[9] This structure was well reproduced in recent density functional theory (DFT) calculations.[7] It was also established,[7] that all transitions in the UV−vis spectrum (250−450 nm) of **1** consist of electron promotions from the five highest occupied molecular orbitals (MOs) to the same doubly degenerate lowest unoccupied MO (LUMO). The latter MOs are characterized as combinations of the σ^*(S−S) and the allylic π^*(NSN) antibonding orbitals.[7] The HOMO of **1** has significant σ(S−S) bonding contribution while the other occupied MOs involved in the discussed transitions are mixtures of essentially nonbonding orbitals localized on S and N atoms. Note, that the first two transitions (λ_{max}^{calc} = 398 and 437 nm) contain significant σ(S−S) → σ^*(S−S) contribution.[7] Thus, the reason for the low energy of these transitions is a small energy gap between σ−bonding and σ^*−antibonding levels, that, in turn, indicates very weak S−S bonds in **1** (Chart 1). Very recently,[10] the S−S bonding interactions in **1** were revealed and visualized by the NCI (noncovalent interactions) analysis and were predicted to be on the order of the hydrogen bonding strength.

Received: January 4, 2012
Published: March 29, 2012

ACS Publications © 2012 American Chemical Society

dx.doi.org/10.1021/ic3000153 | *Inorg. Chem.* 2012, 51, 4747−4755

As there is considerable σ(S−S) → σ^*(S−S) contribution to the lowest singlet excited states of **1**, one might reasonably expect very high photochemical activity of **1**. Indeed, as previously demonstrated,[7] photolysis of hexane solutions of **1** at room temperature results in its decoloration but with a low quantum yield (~0.01). Moreover, Woollins et al.[11] showed that photolysis of **1** in CH_2Cl_2 and MeOH also results in decoloration with formation of cyclic S_7NH in the latter solvent. On the other hand, preparative photolysis of a saturated solution of **1** in cyclohexane gave mainly colored S_4N_2 along with S_7NH, S_8, and some unidentified products.[11]

In contrast to the solution photochemistry, UV irradiation in an Ar matrix at 12 K leads to the transformation of a cage structure of **1** into isomeric structures **2**−**4** (Scheme 1).[7] All of these species (**2**−**4**) have noticeable absorption in the near−UV and visible regions.[7] The primary products of the matrix photochemistry were proposed to be a boat-shaped 8-membered cycle **2** and a novel six-membered S_3N_3 cyclic species **3** carrying an exocyclic (S) −N=S (Scheme 1).[7] On continued UV irradiation both primary intermediates **2** and **3** undergo further transformation to the intermediate **4** (Scheme 1). The latter intermediate could be converted back to the primary products **2** and **3**, as well as to the starting **1**, upon irradiation by visible light (Scheme 1). The findings regarding to **3** and **4** were recently used in the interpretation of electrochemical behavior of **1**.[8]

Scheme 1

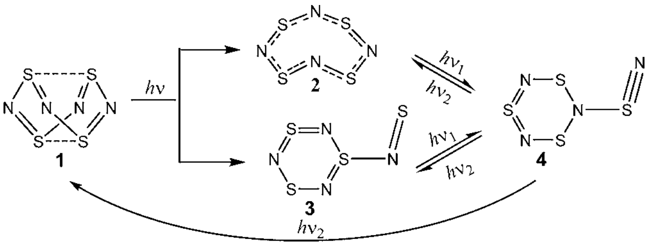

In this paper, we report results of the laser flash photolysis (LFP) studies on the photochemistry of **1** at ambient temperature, along with the high-level quantum chemical calculations. The results of the previous matrix isolation studies[7] facilitated significantly the identification of the intermediates and helped to prove the hypothesis about high photochemical activity of **1**. On the basis of the experimental and computational results, a complete mechanism of the photochemical transformations of **1**, a key compound of the sulfur−nitrogen chemistry, has been proposed and justified.

■ EXPERIMENTAL AND COMPUTATIONAL DETAILS

Compound **1** was synthesized and purified following the published procedure, mp 185−186 °C (decomposition).[12] (***Caution!*** *the compound is explosive*). The UV−vis spectrum of **1** in hexane has an absorption maximum at 254 nm with ε = 1.8 × 10^4 M^{-1} cm^{-1}.

Laser Flash Photolysis (LFP). Two different LFP equipments have been used. A detailed description of the first LFP setup (Novosibirsk) has been published earlier.[13] Solutions, placed in a rectangular cell (inner dimensions 10 mm ×10 mm), were irradiated with a Lambda Physik EMG 101 excimer laser (308 nm, pulse energy up to 100 mJ, pulse duration 15−20 ns) or by the fourth harmonic of a Quanta-Ray LAB-130-10 Nd:YAG laser (266 nm, pulse energy up to 70 mJ, pulse duration 8 ns). The dimensions of the laser beam at the front of the cell were ~3 mm ×8 mm. The monitoring system includes a DKSh-150 xenon short-arc lamp connected to a high current pulser, a homemade monochromator, a 9794B photomultiplier (Electron Tubes Ltd.), and a LeCroy 9310A digitizer. The monitoring light, concentrated in a rectangular of 2.5 mm height and 1 mm width, passed through the cell along the front (laser irradiated) window. Thus, in all experiments the excitation optical length was 1 mm, and the monitoring optical length was 8 mm. The flow system has been used to avoid the effects due to the photoproducts. Some solutions were bubbled with argon or oxygen for 15 min prior to, and during, irradiation. The presence of the dissolved oxygen had no effect on the kinetics and spectroscopy of the detected intermediates.

The quantum yield (φ) of the photorearrangement of **1** at room temperature has been estimated using formation of the 1,10-anthraquinone-1-methide (λ_{max} = 580 nm, ε = 9.25 × 10^3 M^{-1} cm^{-1}, φ_{ac} = 0.8 ± 0.2) upon LFP of 1-methyl-9,10-anthraquinone in ethanol as an actinometric reaction.[14]

Some experiments, including measurements on a millisecond time scale, were performed in Columbus, Ohio.[15] The setup employs a single ARC SP-308 monochromator/spectrograph, with 1-015-300 grating. This model features dual ports, one with a slit and a photomultiplier for kinetic measurements and the other with a flat field and a Roper ICCD-Max 512T Digital ICCD camera for spectroscopic measurements, with up to 2 ns temporal resolution. A Nd:YAG laser (Spectra Physics LAB-150-10, 266 nm, 5 ns, 50 mJ) or XeCl excimer laser (Lambda Physik, 308 nm, ~20 ns, 50 mJ) were used as the excitation light source. Experiments were performed at ambient temperature (~295 K). The sample solutions were changed after every laser shot, unless otherwise indicated.

Quantum Chemical Calculations. As in previous studies,[7] the geometries of **1** and the presumed intermediates of its photolysis were optimized by the B3LYP[16] method using Dunning's correlation-consistent triple-ζ basis set (cc-pVTZ).[17] All of the equilibrium and transition state structures were ascertained to be either minima or saddle points, respectively, on the potential energy surfaces (PES). In addition to second derivative calculations, all transition-state structures were subjected to intrinsic reaction coordinate (IRC) calculations[18] to identify the minima they interconnect.

The Gibbs free energies of the stationary points (minima and transition states) on the PES have been computed in the gas phase using the G3B3 multilevel technique.[19] The Gibbs free energies of solvation have been calculated at the B3LYP/aug-cc-pVTZ//B3LYP/cc-pVTZ level using the PCM[20] model as implemented in the Gaussian 03 suite of programs.[21] To calculate Gibbs free energy in solution, the free energy of solvation was added to the value of the gas phase free energy.

In addition, the Gibbs free energies of **1**−**4** were calculated using another approach, namely, the single-point electronic energies of the proposed intermediates were recalculated using the CCSD(T) procedure[22] with the Dunning's aug-cc-pVTZ basis set with the added d and f functions (2d1f) as proposed previously to account for the inner-shell correlation effects.[23] The Gibbs free energies of solvation were recalculated at the B3LYP/aug-cc-pVTZ(+1d)//B3LYP/cc-pVTZ(+1d) level. Most of calculations were performed with the Gaussian-03 suite of programs.[21] For CCSD(T) calculations, the Gaussian-09 program[24] was employed.

■ RESULTS AND DISCUSSION

LFP of hexane solutions of **1** produces sharp transient absorption with a maximum at 320 nm (Figure 1). However, the shape of the entire spectrum and kinetics of the transient absorption on a nanosecond time scale strongly depend on the laser intensity. Note that similar results were obtained upon both the 266 and the 308 nm laser excitations (Figure 1 and Supporting Information, Figure S1). At low laser intensity, the transient absorption spectrum with almost no absorption in the visible region was formed within the time resolution of the spectrometer and did not change on a nanosecond time scale (Figure 1b, Supporting Information, Figure S1b).

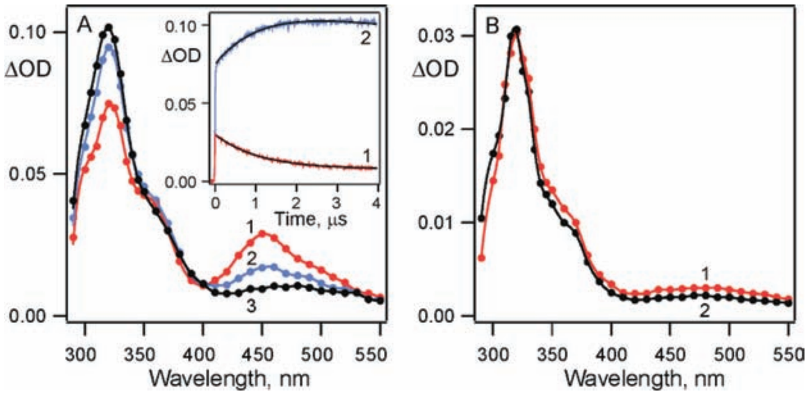

Figure 1. Transient absorption spectra recorded upon excitation of **1** ($c \sim 5.7 \times 10^{-5}$ mol/L) in hexane at ambient temperature by a laser pulse at 266 nm: (A) 1, 2, 3: spectra detected 60 ns, 1, and 3.5 μs after the laser pulse, respectively, with the energy of 52 mJ; Inset: Transient absorption kinetics at 320 nm (1) and 450 nm (2) fitted to biexponential functions (black curves, the second exponent refers to the decay on a time scale of hundred μs and is analyzed below). (B) 1, 2: spectra detected 60 ns and 3.5 μs after the laser pulse with the energy of 5 mJ.

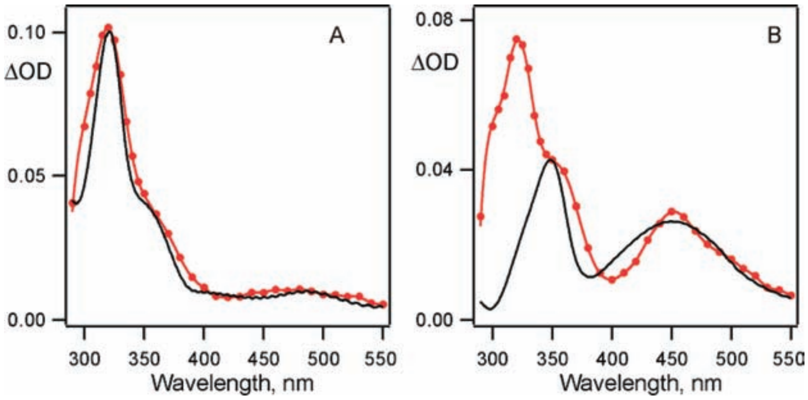

Figure 2. Transient absorption spectra (red curves) recorded upon excitation of **1** ($c \sim 5.7 \times 10^{-5}$ mol/L) in hexane at ambient temperature 3.5 μs (A) and 50 ns (B) after a laser pulse at 266 nm with the energy of 52 mJ. The black traces are the difference absorption UV–vis spectra recorded upon photolysis of **1** in an Ar matrix at 12 K and assigned previously[7] to a mixture of products **2** and **3** (A) and to product **4** (B). The black traces have been adapted from ref 7 and scaled to allow comparison with the LFP spectra.

In contrast to the low laser energy, upon an intense laser excitation (e.g., 52 mJ, Figure 1a), a broad intense visible band ranging from 400 to 550 nm with maximum at 450 nm was formed within a laser pulse and decayed exponentially on a time scale of a few microseconds. The decay of the transient absorption in the visible region was accompanied by the growth of a UV band with maximum near 320 nm. The first order rate constants obtained by the fitting of the decay and growth observed between 290–550 nm coincided and were found to be $k_1 = (1.0 \pm 0.2) \times 10^6$ s^{-1} ($\tau_1 = 1.0 \pm 0.2$ μs). Figure 1 also demonstrates that the spectrum formed 3.5 μs after the intense laser excitation is very similar to that formed without time delay upon low energy pulse.

All aforementioned experimental findings can be easily explained using the results of the previously reported matrix study.[7] As mentioned in the Introduction, compounds **2** and **3** are most likely the primary products of the photochemical transformation of **1** in an Ar matrix at 12 K (Scheme 1), but on further irradiation both can be easily converted to the isomer **4**.[7] The former two species absorb mainly in the near-UV region with maximum at about 320 nm, their absorption in the visible region is very low. On the other hand, isomer **4** has an intense absorption band at 450 nm along with a band at 350 nm.[7] Similar to the matrix photochemistry, excitation of **1** in solution at ambient temperature leads to formation of the species **2** and **3**. At high laser intensity, the primary products **2** and **3** absorb a second photon and undergo transformation to the isomer **4**. The isomer **4** is very unstable and converts back to **2** or **3** (or both of them).

Indeed, the transient absorption spectrum detected 3.5 μs after an intense laser pulse is very close to the difference absorption UV–vis spectrum of a mixture of compounds **2** and **3** in an Ar matrix (Figure 2a).[7] In turn, comparison of the transient absorption recorded 50 ns after the intense laser pulse with the difference absorption spectrum of **4** (Figure 2b) clearly shows that it is a compound that undergoes reaction with rate constant $k_1 = 10^6$ s^{-1}.

At low laser intensity, LFP of **1** leads to formation of a mixture of **2** and **3**. Formation of **2** requires dissociation of the weak trans-annular S–S bonds of **1**. In turn, formation of **3** requires dissociation of an S–N bond, followed by a recyclization. The latter photochemical reaction is typical of sulfur–nitrogen heterocyclic compounds.[2c,25] To test the prediction of a large photochemical activity of S_4N_4, we performed a very rough estimation of the quantum yield of the product formation. The effective extinction coefficient at 320 nm (ε_{eff}^{320}) of a mixture of **2** and **3** formed upon photolysis of **1** in an argon matrix was roughly estimated as $\sim 8 \times 10^3$ M^{-1} cm^{-1}. The same composition of the primary products **2** and **3** was proposed to be formed at cryogenic and ambient temperatures, and the quantum yield of their formation was estimated as

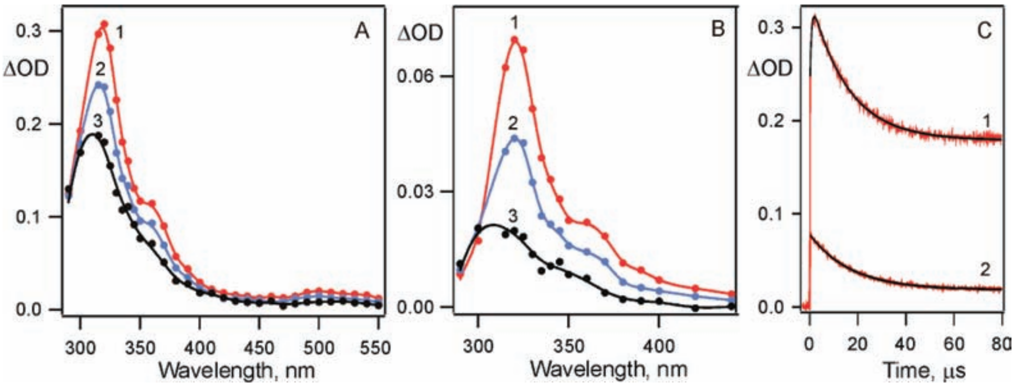

Figure 3. Transient absorption spectra recorded upon excitation of **1** ($c \sim 5.0 \times 10^{-4}$ mol/L) in hexane at ambient temperature 3 μs (1), 15 μs (2), and 75 μs (A and B) after a laser pulse at 308 nm with the energy of 60 mJ (A) and 5 mJ (B). (C) Transient absorption kinetics (red curves) at 320 nm recorded for the laser pulse energies of 60 (1) and 5 mJ (2) fitted to a biexponential (1, first exponent refers to the formation of **2** and **3** from **4** with $k = 10^6$ s^{-1}) and exponential (2) functions (black curves).

0.9 ± 0.2 in hexane at ambient temperature (Supporting Information, Figure S2). As the quantum yield of photodegradation is low (~0.01), the intermediates **2** and **3** undergo almost exclusive isomerization to the starting compound **1**.

The transient absorption spectra assigned to the mixture of intermediates **2** and **3** (Figure 3A and 3B, spectrum 1) decay exponentially on the microsecond time scale (Figure 3C). The rate constant of this decay (k_2) was found to be independent of laser intensity and excitation wavelength (266 and 308 nm) and equal to $(6.7 \pm 1.0) \times 10^4$ s^{-1} ($\tau_2 = 15 \pm 2$ μs). However, the ratio of optical densities at the beginning and end of this decay depends noticeably on the laser intensity (Figure 3C, Supporting Information, Figure S3), being equal to 1.7 and 4.0 at 60 and 5 mJ, respectively. It means that different compositions of intermediates **2** and **3** are formed in these cases. At high laser intensity, the contribution of the long-lived intermediate is significantly higher. This fact can be easily explained if one posits that intermediate **4** is formed photochemically from both primary products (as was observed in Ar matrix[7]), but that it converts preferentially to the longer-lived intermediate (**2** or **3**).

The transient absorption spectrum of the long-lived intermediate with a maximum at ~310 nm decays exponentially on a millisecond time scale (Figure 4) with a rate constant $k_3 = (2.8 \pm 0.2) \times 10^2$ s^{-1} ($\tau_3 = 3.6 \pm 0.3$ ms).

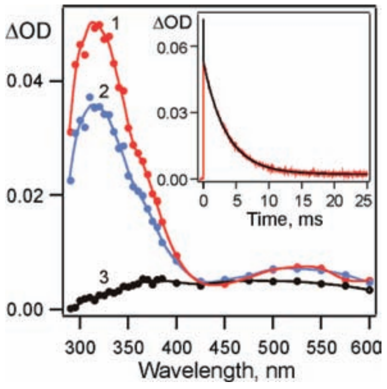

Figure 4. Transient absorption spectra recorded upon excitation of **1** ($c \sim 6.9 \times 10^{-5}$ mol/L) in hexane at ambient temperature 200 μs (1), 1.5 ms (2) and 75 ms after a laser pulse at 266 nm. Inset: Transient absorption kinetics at 320 nm (red curve) fitted to a biexponential function (black curve, first exponent refers to a decay presented in Figure 3C).

To assign kinetic processes with time constants 15 μs and 3.6 ms to decay of specific intermediates (**2** or **3**), we analyzed the decay associated spectra (DAS) (Figures 5 and 6). The DAS corresponding to the intermediate with a 15 μs lifetime is in perfect agreement with the difference UV–vis spectrum detected previously[7] in an Ar matrix (Figure 5) and assigned to compound **2** on the basis of IR spectroscopy. In addition, Figure 6A shows that this DAS is in good agreement with the calculated UV–vis spectrum of compound **2**.

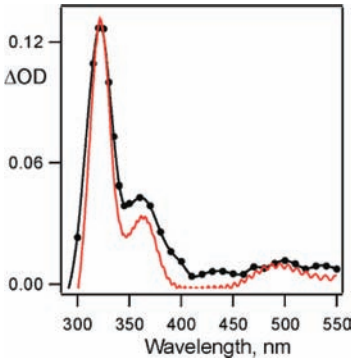

Figure 5. Decay associated spectrum (DAS) related to a species with 15 μs lifetime (black points) and difference UV–vis spectrum recorded in argon matrix at 12 K and assigned to the species **2** (red spectrum). The latter spectrum has been adapted from the Supporting Information for ref 7. Copyright 2009 American Chemical Society.

In turn, the DAS corresponding to the long-lived species (3.6 ms) is in better agreement with the UV–vis spectrum calculated for compound **3** (Figure 6B). Indeed, this DAS spectrum is characterized by a broad absorption band in the 300–400 nm range, which is consistent with a series of electronic transitions in the calculated spectrum of **3**.

As a whole, Figure 6 demonstrates that the predicted absorption spectra of the isomers **2** and **3** are in very good agreement with experiment. Agreement could be even better if one considers the bleaching of the starting material **1** (Figure 6A, Inset), which shifts slightly the DAS spectra to the red compared to the normal UV–vis spectra. Calculations predict also (Supporting Information, Figure S4) that extinction coefficients at the maxima of the absorption bands of **2** and **3** at about 320 nm are similar (15.5×10^3 and 9.2×10^3 M^{-1} cm^{-1} for **2** and **3**, respectively). Moreover, these values

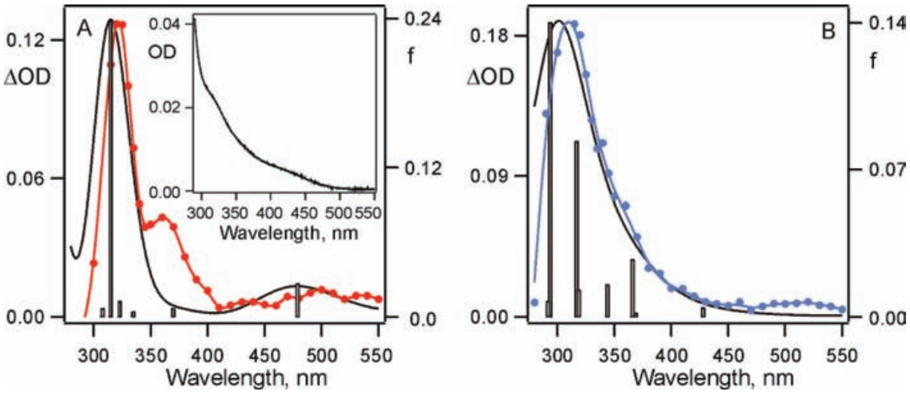

Figure 6. Decay associated spectra (DAS) obtained for **1** in hexane at ambient temperature: components associated with 15 μs (A) and 3.6 ms (B) lifetimes. Inset: UV−vis spectrum of **1** (c = 1.2 × 10^{-5} mol/L). The electronic transitions in the UV−vis spectra[7] calculated at the time dependent B3LYP/aug-cc-pVTZ level are depicted as a sum of Gaussians (black spectra) and as vertical bars (positions and oscillator strengths, f) for compounds **2** (A) and **3** (B).

are in reasonable agreement with the effective extinction coefficient estimated for a mixture of **2** and **3** produced by irradiation in an Ar matrix ($\varepsilon_{eff}^{320} \sim 8 \times 10^3$ M^{-1} cm^{-1}). On the basis of these calculations, the comparable yields of the primary products **2** and **3** (although with some preference for **2**) can be proposed. The use of a high intensity laser beam leads to a significant increase in the yield of product **3** (Supporting Information, Figure S3). However, both products are unstable and undergo conversion back to **1**.

Thus, we revealed that **1** is a photochromic compound undergoing in solution the thermally reversible photochemical isomerization. Scheme 2 represents the mechanism of the photochromic transformations of S_4N_4. The rate constants of the elementary reactions are presented in Table 1.

Scheme 2

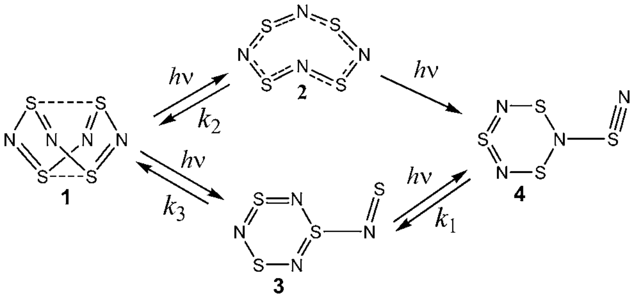

Table 1. Experimental Rate Constants (k_{exp}) of the Elementary Reactions (Scheme 2) Measured in Hexane at Ambient Temperature (∼295 K) and Calculated (k_{calc}) According Formulae (1) Using Results of G3B3 Calculations (heptane, 298 K)

	k_1, s^{-1}	k_2, s^{-1}	k_3, s^{-1}
k_{exp}	(1.0 ± 0.2) × 10^6	(6.7 ± 1.0) × 10^4	280 ± 20
k_{calc} (G3B3)	3 × 10^7	1 × 10^6	28

In a previous paper,[7] we demonstrated that DFT calculations at the B3LYP/cc-pVTZ level reproduce very well the IR spectra of **1** and its isomers **2**−**4**, which indicates that this level of theory is well suited for geometry optimization. Indeed, as mentioned in the Introduction, the geometry of **1** optimized at this level is very close to those determined experimentally in the crystalline state and in the gas phase.[9] Moreover, a boat structure of isomer **2** resembles that of the N-bonded adducts of **1** with some Lewis acids (e.g., $SbCl_5$).[1b,26] The thermodynamics of the discussed reactions (Schemes 1 and 2) has been also calculated at the same level.[7] Unfortunately, results of the DFT calculations[7] do not agree with the experimental findings of this paper. For example, compounds **1** and **2** were predicted to be very close in energy (ΔH_{rel} = 0.4 kcal/mol).[7] Similar formation enthalpies were also predicted for **3** and **4** (ΔH_{rel} = 1.1 kcal/mol).[7] According to the LFP data, **1** is thermodynamically the most preferable isomer, while isomer **4** is the least favorable one.

Therefore, we recalculated the single-point electronic energies of the proposed intermediates using the CCSD(T) procedure with a very large basis set (Dunning's aug-cc-pVTZ basis set with the added d and f functions, 2d1f). Figure 7 demonstrates that at this level of theory the boat structure **2** is predicted to be significantly less favorable than cage structure **1**. In addition, the most reactive intermediate **4** has the highest enthalpy of formation and Gibbs free energy at this level of

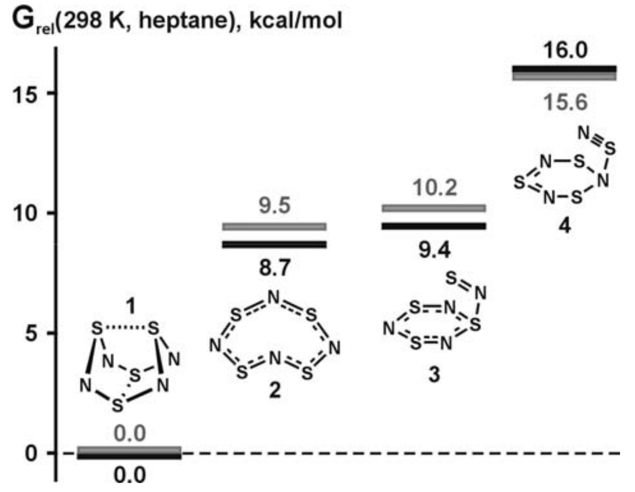

Figure 7. Relative Gibbs free energies in heptane at 298 K of **1** and its isomers **2**−**4** calculated at the CCSD(T)/aug-cc-pVTZ(+2d1f)//B3LYP/cc-pVTZ(+d) (gray lines) and G3B3 (black lines) levels of theory.

theory. Calculations at the G3B3 level gave similar results (Figure 7).

We employed the G3B3 approach to analyze the mechanism of thermal transformations presented in Scheme 2 and to calculate the rate constants of elementary steps. The rate constants of monomolecular reactions were computed in accordance with the canonical transition state theory (TST):

$$k(T) = \alpha \frac{kT}{h} \exp\left(-\frac{\Delta G^{\ddagger}(T)}{kT} \right) \tag{1}$$

where α is a statistical factor (a number of equivalent reaction channels) and $\Delta G^{\ddagger}$ is a free energy of activation.

On the basis of the experimental results, we hypothesized that isomer **4** converts preferentially to the long-lived intermediate **3**. Three pathways were found for this transformation (Supporting Information, Figure S5): a one-step isomerization of **4′** (the rotamer of **4**) with migration of SN substituent (A), a two−step reaction with formation of a new intermediate six-membered S_3N_3 cyclic species (**5**, Chart 2) carrying exocyclic (S)-S≡N (B), and a two−step reaction with formation of five-membered S_3N_2 cyclic species (**6**, Chart 2) carrying exocyclic (S)=N−S≡N (C). Transition states (TSs) for all these reactions have been localized and IRC calculations have demonstrated that they interconnect correct minima.

Chart 2

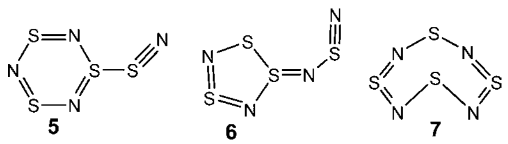

The former route (Supporting Information, Figure S5A and Figure 8) was found to be preferential as it has the lowest TS and, thus, the highest rate constant which was predicted to be 3×10^7 s^{-1}. This value is noticeably higher than the experimental one (Table 1), and the reason for this could be insufficient accuracy of the level of theory employed. For example, calculations at the CCSD(T)/aug-cc-pVTZ(+2d1f)//B3LYP/cc-pVTZ(+d) level predict a significantly lower rate constant (2×10^5 s^{-1}) in better agreement with experiment.

For this reaction, the calculations predict a loose transition state with very long breaking and forming N−S bonds (Figure 8, TS2). At the same time, the distances between the sulfur atom of the migrating NS group and the two sulfur atoms of the ring (2.71 Å, Figure 8) are about 0.9 Å shorter than the sum of their van der Waals radii, indicating significant bonding interactions. Thus, the geometry of TS2 resembles a complex of two radicals ($S_3N_3^{\bullet}$ and $NS^{\bullet}$). Note, that the $S_3N_3^{\bullet}$ radical has never been identified in condensed phase.[8,27] However, it has been detected by photoelectron spectroscopy upon vaporization of $[SN]_x$ polymer.[28]

Most likely, this reaction can be viewed as "roaming-mediated isomerization",[29] exemplified by nitromethane and nitrobenzene dissociation.[30] A very loose transition state of biradical nature has been located for the nitro-nitrite isomerization followed by the dissociation of methylnitrite ($CH_3NO_2 \rightarrow CH_3ONO \rightarrow CH_3O + NO$).[30a] In contrast to the nitromethane isomerization,[30a] a loose transition state of Figure 8 has a closed-shell electronic configuration: the restricted singlet state wave function of the TS2 is stable. We have also analyzed the multireference character of the wave function of TS2 using the T1 diagnostic for the CCSD calculation.[31] Modest T1 value obtained in this case (0.023) indicates that a single reference-based electron correlation procedure is appropriate in the present case.[31]

We have also considered the thermal transformation of intermediates **2** and **3** to the cage structure (**2** → **1** and **3** → **1**). We were unable to localize transition states for one−step reactions. Both conversions have been predicted to proceed in two steps (Figures 9 and 10). A very shallow minimum was localized on the potential energy surface (PES) for the rearrangement of **2** into **1** (Figure 9). The 8-membered cyclic structure with four nitrogen atoms lying in the plane corresponds to this minimum (**7**, Chart 2). Note that four sulfur atoms are in the plane in the case of structure **2**. The rate constant of the compound **2** decay (k_2) was calculated using results of Figure 9 and the steady state approximation for the concentration of intermediate **7**. Similar to the previous case, calculations overestimate the rate constant by more than order of magnitude (Table 1).

In agreement with experiment, species **3** is predicted to be the less reactive intermediate (Figure 10). A two-step reaction of **3** proceeds through the formation of the intermediate **6**

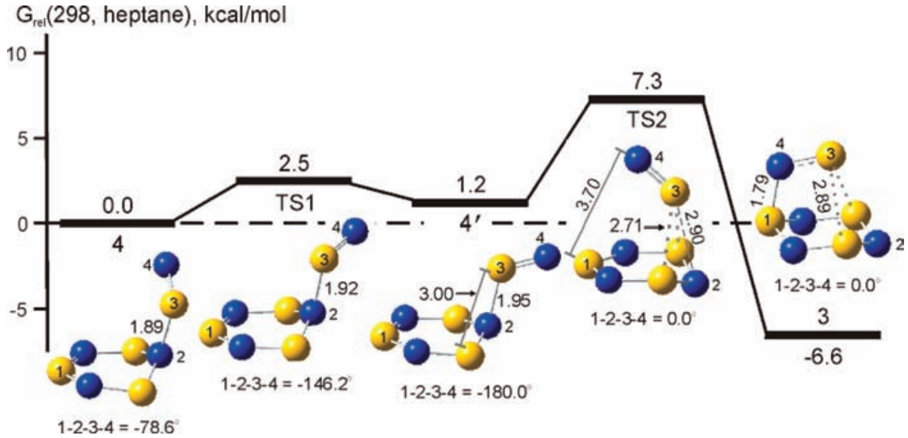

Figure 8. Relative Gibbs free energies in heptane at 298 K of the species involved in the isomerization of the cyclic species **4** to cyclic species **3** calculated at the G3B3 level. Structures of the intermediates and transition states optimized at the B3LYP/6-31G(d) level with selected bond lengths, interatomic distances, and dihedral angles (S, yellow; N, blue).

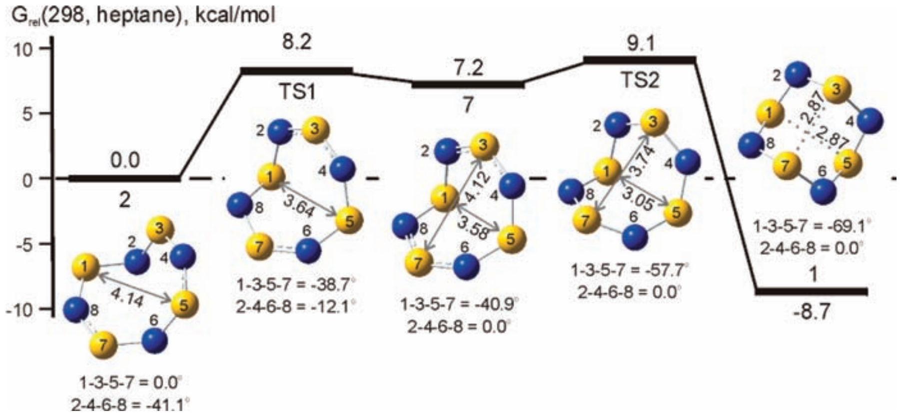

Figure 9. Relative Gibbs free energies in heptane at 298 K of the species involved in the transformation of the boat-shaped 8-membered cycle **2** to the cage structure **1**, calculated at the G3B3 level. Structures of the intermediates and the transition states optimized at the B3LYP/6-31G(d) level with selected bond lengths, interatomic distances, and dihedral angles (S, yellow; N, blue).

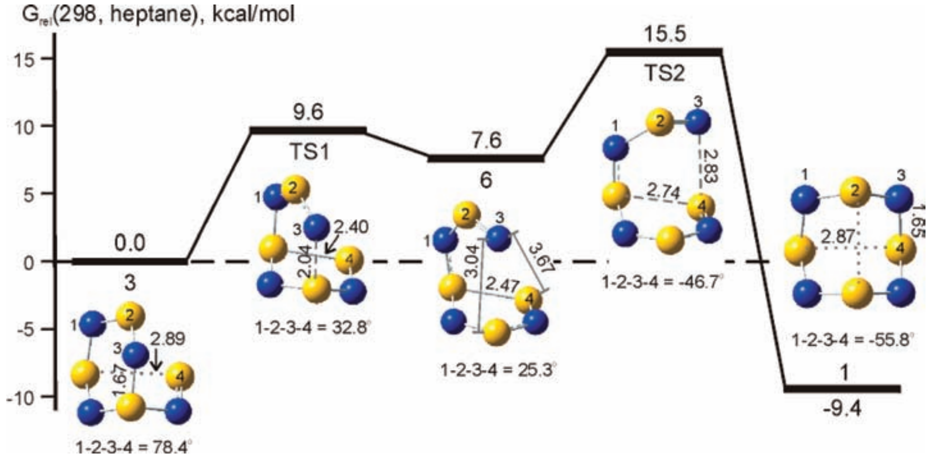

Figure 10. Relative Gibbs free energies in heptane at 298 K of the species involved in the transformation of the six-membered cyclic species **3** to the cage structure **1**, calculated at the G3B3 level. Structures of the intermediates and the transition states optimized at the B3LYP/6-31G(d) level with selected bond lengths, interatomic distances, and dihedral angles (S, yellow; N, blue).

discussed above (Supporting Information, Figure S4). The rate constant of the compound **3** decay (k_3) calculated using results of Figure 10 is equal to 28 s^{-1}. In contrast to the previous two reactions, the rate constant of the latter reaction is underestimated by about 1 order of magnitude (Table 1).

Therefore, the calculations are in qualitative agreement with experiment and predict the rate constants of the discussed thermal rearrangements to within an order of magnitude. Most importantly, the results of the calculations support the assignment of the spectra recorded experimentally. Indeed, according to the calculations, the most reactive is intermediate **4** and the most long-lived is intermediate **3**. Overall, the results of the calculations confirm the mechanism of photochromic transformation of **1**, shown in Scheme 2.

As discussed in the Introduction, **1** absorbs visible light (Figure 6A, Inset). Thus, the photochemical formation of compounds **2** and **3** could not be excluded in the course of inorganic and organoelement syntheses with participation of **1**. The long-lived thionitroso compound **3** is likely a very reactive species. Nowadays, relatively little is known about chemistry of thionitroso compounds (R−N═S).[32] Some metal-stabilized derivatives were isolated.[33] A few thionitrosoalkanes[34] and thionitrosoarenes[35] have been generated and intercepted in Diels−Alder and some other pericyclic reactions.[36] Nevertheless, it is clear that R−N═S compounds are highly reactive, and that this reactivity could be responsible, at least in part, for the varied chemical properties of **1**.

■ ASSOCIATED CONTENT

Ⓢ Supporting Information

Spectra and kinetics of LFP studies, dependence of the transient absorption on the energy of the laser pulse, and details of the quantum chemical calculations. This material is available free of charge via the Internet at http://pubs.acs.org.

■ AUTHOR INFORMATION

Corresponding Author

*E-mail: gritsan@kinetics.nsc.ru.

Notes

The authors declare no competing financial interest.

■ ACKNOWLEDGMENTS

The authors are grateful to the Russian Foundation for Basic Research (projects 07-03-00467, 10-03-00735) and the Presidium of the Russian Academy of Sciences (project 8.14) for financial support. The support of this work by the Ohio and the Siberian Supercomputer Centers is also gratefully acknowledged.

■ REFERENCES

(1) (a) Chivers, T.; Laitinen, R. S. In *Handbook of Chalcogen Chemistry. New Perspectives in Sulfur, Selenium and Tellurium*; Devillanova, F., Ed.; RSC Press: Cambridge, U.K., 2007. (b) Chivers, T. *A Guide to Chalcogen-Nitrogen Chemistry*; World Scientific: London, U.K., 2005. (c) Greenwood, N. N.; Earnshaw, A. *Chemistry of the Elements*; Butterworth-Heinemann: Oxford, U.K., 1997, pp 721−746. (d) Chivers, T. In *Encyclopedia of Inorganic Chemistry*; Wiley, Chichester, 1994, Vol. 7.

(2) (a) Hicks, R. G. In *Stable Radicals: Fundamentals and Applied Aspects of Odd-Electron Compounds*; Hicks, R. G., Ed.; Wiley: New York, 2010. (b) Zibarev, A. V.; Mews, R. In *Selenium and Tellurium Chemistry: From Small Molecules to Biomolecules and Materials*; Woollins, J. D., Laitinen, R. S., Eds.; Springer Verlag: Berlin, Germany, 2011. (c) Gritsan, N. P.; Makarov, A. Yu.; Zibarev, A. V. *Appl. Magn. Reson.* **2011**, *4*, 449−466. (d) Gritsan, N. P.; Zibarev, A. V. *Russ. Chem. Bull.* **2011**, *60*, 2127−2136.

(3) (a) Rawson, J. M.; Alberola, A. In *Handbook of Chalcogen Chemistry. New Perspectives in Sulfur, Selenium and Tellurium*; Devillanova, F., Ed.; RSC Press: Cambridge, U.K., 2007. (b) Rawson, J. M.; Alberola, A.; Whalley, A. *J. Mater. Chem.* **2006**, *16*, 2560−2575. (c) Rawson, J. M.; Luzon, J.; Palacio, F. *Coord. Chem. Rev.* **2005**, *249*, 2631−2641. (d) Boere, R. T.; Roemmele, T. L. *Coord. Chem. Rev.* **2000**, *210*, 369−445. (e) Rawson, J. M.; Palacio, F. *Struct. Bond. (Berlin)* **2001**, *100*, 93−128. (f) Rawson, J. M.; McManus, G. D. *Coord. Chem. Rev.* **1999**, *189*, 135−168.

(4) (a) Winter, S. M.; Datta, S.; Hill, S.; Oakley, R. T. *J. Am. Chem. Soc.* **2011**, *133*, 8126−8129. (b) Leitch, A. A.; Lekin, K.; Winter, S. M.; Downie, L. E.; Tsuruda, H.; Tse, J. S.; Mito, M.; Desgreniers, S.; Dube, P. A.; Zhang, S.; Liu, Q.; Jin, C.; Ohishi, Y.; Oakley, R. T. *J. Am. Chem. Soc.* **2011**, *133*, 6051−6060. (c) Yu, X.; Mailman, A.; Dube, P. A.; Assoud, A.; Oakley, R. T. *Chem. Commun.* **2011**, *47*, 4655−4657. (d) Lekin, K.; Winter, S. M.; Downie, L. E.; Bao, X.; Tse, J. S.; Desgreniers, S.; Secco, R. A.; Dube, P. A.; Oakley, R. T. *J. Am. Chem. Soc.* **2010**, *132*, 16212−16224. (e) Tse, J. S.; Leitch, A. A.; Yu, X.; Bao, X.; Zhang, S.; Liu, Q.; Jin, C.; Secco, R. A.; Desgreniers, S.; Ohishi, Y.; Oakley, R. T. *J. Am. Chem. Soc.* **2010**, *132*, 4876−4886.

(5) (a) Clarke, C. S.; Jornet-Somoza, J.; Mota, F.; Novoa, J. J.; Deumal, M. *J. Am. Chem. Soc.* **2010**, *132*, 17817−17830. (b) Deumal, M.; Rawson, J. M.; Howard, J. A. K.; Copley, R. C. B.; Robb, M. A.; Novoa, J. J. *Chem.—Eur. J.* **2010**, *16*, 2741−2750. (c) Deumal, M.; LeRoux, S.; Rawson, J. M.; Robb, M. A.; Novoa, J. J. *Polyhedron* **2007**, *26*, 1949−1958. (d) Awaga, K.; Tanaka, T.; Shirai, T.; Umezono, Y.; Fujita, W. *C. R. Chim.* **2007**, *10*, 52−57. (e) Preuss, K. E. *Dalton Trans.* **2007**, 2357−2369.

(6) (a) Torroba, T. *J. Prakt. Chem.* **1999**, *341*, 99−113. (b) Rees, C. W. *J. Heterocyclic Chem.* **1992**, *29*, 639−651.

(7) Pritchina, E. A.; Gritsan, N. P.; Bally, T.; Zibarev, A. V. *Inorg. Chem.* **2009**, *48*, 4075−4082.

(8) Boere, R. T.; Chivers, T.; Roemmele, T. L.; Tuononen, H. M. *Inorg. Chem.* **2009**, *48*, 7294−7306.

(9) (a) Sharma, B. D.; Donohue, J. *Acta Crystallogr.* **1963**, *16*, 891−897. (b) DeLucia, M. L.; Coppens, P. *Inorg. Chem.* **1978**, *17*, 2336−2338. (c) Almond, M. J.; Forsyth, G. A.; Rice, D. A.; Downs, A. J.; Jeffery, T. L.; Hagen, K. *Polyhedron* **1989**, *8*, 2631−2636. (d) Irsen, S. H.; Jacob, P.; Dronskowski, R. *Z. Anorg. Allg. Chem.* **2001**, *627*, 321−325. (e) Chung, G.; Lee, D. *J. Mol. Struct.: THEOCHEM* **2002**, *582*, 85−90.

(10) Contreras-Garcha, J.; Johnson, E. R.; Keinan, S.; Chaudret, R.; Piquemal, J.-P.; Beratan, D. N.; Yang, W. *J. Chem. Theory Comput.* **2011**, *7*, 625−632.

(11) Allen, C. W.; Kelly, P. F.; Woollins, J. D. *J. Chem. Soc., Dalton Trans.* **1991**, 1343−1345.

(12) (a) Villena-Blanco, M.; Jolly, W. L. *Inorg. Synth.* **1967**, *9*, 98−102. (b) Makarov, A. Yu.; Bagryanskaya, I. Yu.; Gatilov, Yu. V.; Mikhalina, T. M.; Shakirov, M. M.; Shchegoleva, L. N.; Zibarev, A. V. *Heteroatom. Chem.* **2001**, *12*, 563−576. (c) Maaninen, A.; Siivari, J.; Laitinen, R. S.; Chivers, T. *Inorg. Synth.* **2002**, *33*, 196−199.

(13) Tsentalovich, Yu. P.; Kulik, L. V.; Gritsan, N. P.; Yurkovskaya, A. V. *J. Phys. Chem. A* **1998**, *102*, 7975−7980.

(14) (a) Gritsan, N. P.; Khmelinski, I. V.; Usov, O. M. *J. Am. Chem. Soc.* **1991**, *113*, 9615−9620. (b) Gritsan, N. P.; Rogov, V. A.; Bazhin, N. M.; Russkikh, V. V.; Fokin, E. P. *Teor. Eksp. Khim.* **1979**, *15*, 290−296. (c) Gritsan., N. P.; Bazhin, N. M. *Izv. Sib. Otd. Akad. Nauk SSSR* **1979**, 138−143.

(15) (a) Martin, C. B.; Shi, X.; Tsao, M.-L.; Karweik, D.; Brooke, J.; Hadad, C. M.; Platz, M. S. *J. Phys. Chem. B* **2002**, *106*, 10263−10271. (b) Tsao, M.-L.; Gritsan, N. P.; James, T. R.; Platz, M. S.; Hrovat, D.; Borden, W. T. *J. Am. Chem. Soc.* **2003**, *125*, 9343−9358.

(16) (a) Becke, A. D. *J. Chem. Phys.* **1993**, *98*, 5648−5652. (b) Lee, C.; Yang, W.; Parr, R. G. *Phys. Rev. B* **1988**, *37*, 785−789.

(17) Dunning, T. H. *J. Chem. Phys.* **1989**, *90*, 1007−1023.

(18) Gonzalez, C.; Schlegel, H. B. *J. Chem. Phys.* **1989**, *90*, 2154−2161.

(19) Baboul, A. G.; Curtiss, L. A.; Redfern, P. C.; Raghavachari, K. *J. Chem. Phys.* **1999**, *110*, 7650−7657.

(20) Tomasi, J.; Mennucci, B.; Cammi, R. *Chem. Rev.* **2005**, *105*, 2999−3093.

(21) Frisch, M. J. A.;et al. *Gaussian 03*, Revision B.01; Gaussian, Inc.: Pittsburg, PA, 2003 (Full reference is given in the Supporting Information).

(22) (a) Cizek, J. *Adv. Chem. Phys.* **1969**, *14*, 35−89. (b) Purvis, G. D.; Bartlett, R. J. *J. Chem. Phys.* **1982**, *76*, 1910−1918.

(23) (a) Bauschlicher, C. W.; Partridge, H. *Chem. Phys. Lett.* **1995**, *240*, 533−540. (b) Martin, J. M. L. *Chem. Phys. Lett.* **1995**, *242*, 343−350.

(24) Frisch, M. J. A.;et al. *Gaussian 09*, Revision A.01; Gaussian, Inc.: Wallingford, CT, 2009 (Full reference is given in Supporting Information).

(25) (a) Shuvaev, K. V.; Bagryansky, V. A.; Gritsan, N. P.; Makarov, A. Yu.; Molin, Yu. N.; Zibarev, A. V. *Mendeleev Commun.* **2003**, *13*, 178−179. (b) Gritsan, N. P.; Kim, S. N.; Makarov, A.Yu.; Chesnokov, E. N.; Zibarev, A. V. *Photochem. Photobiol. Sci.* **2006**, *5*, 95−101. (c) Gritsan, N. P.; Shuvaev, K. V.; Kim, S. N.; Knapp, C.; Mews, R.; Bagryansky, V. A.; Zibarev, A. V. *Mendeleev Commun.* **2007**, *17*, 204−206.

(26) (a) Neubauer, D.; Weiss, J. *Z. Anorg. Allg. Chem.* **1960**, *303*, 28−38. (b) Chivers, T.; Hilts, R. W. *Coord. Chem. Rev.* **1994**, *137*, 201−232. (c) Konu, J.; Bajorek, T.; Laitinen, R. S.; Chivers, T.; Suontamo, R. J.; Ahlgren, M. *Eur. J. Inorg. Chem.* **2006**, 2951−2958.

(27) Boere, R. T.; Tuononen, H. M.; Chivers, T.; Roemmele, T. L. *J. Organomet. Chem.* **2007**, *692*, 2683−2696.

(28) (a) Lau, W. M.; Westwood, N. P. C.; Palmer, M. H. *J. Chem. Soc., Chem. Commun.* **1985**, 752−753. (b) Lau, W. M.; Westwood, N. P. C.; Palmer, M. H. *J. Am. Chem. Soc.* **1986**, *108*, 3229−3237.

(29) Herath, N.; Suits, A. G. *J. Phys. Chem. Lett.* **2011**, *2*, 642−647.

(30) (a) Zhu, R. S.; Lin, M. C. *Chem. Phys. Lett.* **2009**, *478*, 11−16. (b) Hause, M. L.; Herath, N.; Zhu, R. S.; Lin, M. C.; Suits, A. G. *Nat. Chem.* **2011**, *3*, 932−937.

(31) (a) Bauschlicher, C. W.; Partridge, H. *Chem. Phys. Lett.* **1995**, *240*, 533−540. (b) Martin, J. M. L. *Chem. Phys. Lett.* **1995**, *242*, 343−350.

(32) (a) Takahashi, M.; Okazaki, R. *Sulfur Rep.* **1993**, *13*, 293−338. (b) Reed, M. G.; Zhang, D. Y. *J. Mol. Struct.: THEOCHEM* **2001**, *548*, 107−112.

(33) Otsuka, S.; Yoshida, T.; Nakamura, A. *Inorg. Chem.* **1968**, *7*, 1833−1835.

(34) (a) Hata, Y.; Watanabe, M. *J. Org. Chem.* **1980**, *45*, 1691−1692. (b) Bryce, M. R.; Chesney, A.; Heaton, J. N.; McKelvey, J. N.; Anderson, M. *Tetrahedron Lett.* **1994**, *25*, 5275−5278.

(35) (a) Davis, F. A.; Skibo, E. B. *J. Org. Chem.* **1976**, *41*, 1333−1336. (b) Pedersen, C. L.; Lohse, C.; Poliakoff, M. *Acta Chem. Scand. B* **1978**, *32*, 625−631. (c) Mayer, R.; Domschke, G.; Bleisch, S.; Bartl, A. *Tetrahedron Lett.* **1978**, *19*, 4003−4006. (d) Pedersen, C. L.; Lohse, C.; Poliakoff, M. *Acta Chem. Scand. B* **1978**, *32*, 625−631. (e) Joucla, M. F.; Rees, C. W. *Chem. Commun.* **1984**, 374−375. (f) Okazaki, R.; Takahashi, M.; Inamoto, N.; Sugawara, T.; Iwamura, H. *Chem. Lett.*

1989, *12*, 2083−2086. (g) Takahashi, M.; Okazaki, R.; Inamoto, N. *Chem. Lett.* **1989**, *12*, 2087−2090. (h) Takahashi, M.; Okazaki, R.; Inamoto, N.; Sugawara, T.; Iwamura, H. *J. Am. Chem. Soc.* **1992**, *114*, 1830−1837. (i) Bryce, M. R.; Heaton, J. N.; Taylor, P. C.; Anderson, M. *J. Chem. Soc. Perkin Trans. 1* **1994**, 1935−1944.

(36) (a) Le, T. N.; Nguen, L. T.; Chandra, A. K.; De Proft, F.; Geerlink, P.; Nguen, M. T. *J. Chem. Soc., Perkin Trans. 2* **1999**, 1249−1255. (b) Sperling, D.; Mehlhorn, A.; Reissig, H.-U.; Fabian, J. *Liebigs Annalen* **1996**, 1615−1621.